The evolution of gynodioecy on a lattice

T. Preece, Y. Mao

Author's Accepted Manuscript

www.elsevier.com/locate/yjtbi

Cite this article as: T. Preece and Y. Mao, The evolution of gynodioecy on a lattice, *Journal of Theoretical Biology*, doi:10.1016/j.jtbi.2010.06.025

The evolution of gynodioecy on a lattice

T. Preece*, Y. Mao

School of Physics and Astronomy, University of Nottingham, University Park, Nottingham NG7 2RD, United Kingdom

Abstract

Gynodioecy is a breeding system in plants where populations consist of hermaphrodites and females. The females result from a genetic mutation which impairs pollen production in hermaphrodite plants. Most previous models for the evolution of gynodioecy do not take into account any spatial detail, which might be expected to play an important role in populations with short range interactions caused by poor or no locomotion.

In this article we present a generalised mean-field analysis (which ignores any spatial detail), together with stochastic spatial simulations, to investigate the spatial effect on the evolution of gynodioecy. We show that, in a population of hermaphrodites where male sterility is caused by a dominant allele in a nuclear gene, mean-field calculations greatly underestimate the reproductive advantage females require to become viable under spatial constraints. This suggests that gynodioecy is less likely to evolve in plants with more localised pollination and seed setting. This may have implications for the evolution of dioecy, a breeding system in plants where the population consists of males

---

*Corresponding author
Email addresses: ppxtp@nottingham.ac.uk (T. Preece),
yong.mao@nottingham.ac.uk (Y. Mao)

and females, as gynodioecy is thought to be a route to dioecy. Our results also demonstrate that a lower frequency of females should be expected for gynodioecious populations when interactions are local. This is relevant when comparing the results of breeding experiments with observations of female frequency in the wild.

Key words: sexual reproduction, lattice, Gynodioecy

---

1. Introduction

Gynodioecy is a breeding system in plants where populations consist of hermaphrodite and female individuals. It is both a common and widespread polymorphism describing approximately 7% of all flowering plants (Richards, 1986). Some examples of species that exhibit gynodioecy are the wild strawberry, *Fragaria virginiana*, (Ashman, 1999) and *Cucurbita foetidissima* (Cucurbitaceae) (Kohn, 1989). The evolution of gynodioecy also has implications for the evolution of dioecy, as gynodioecy is thought to be a route to dioecy. A well-known dioecious species is American holly, *Ilex aquifolium* (Aquifoliaceae) (Obeso et al., 1998).

Gynodioecy occurs as a result of a genetic mutation which impairs pollen production in hermaphrodite plants. This makes gynodioecy an excellent system for studying the interplay of genetic architecture and ecology in evolution (Bailey and Delph, 2007). Genetic mutations can impair pollen production in several ways but still allow normal female reproduction (Chaudhury, 1993). The genetic basis for male sterility can significantly affect whether a mutation for male sterility can become established. Nuclear genes are inherited through both parents whereas cytoplasmic genes are only inherited from the

2

mother. It has been shown that females would need to be at least twice as fertile as hermaphrodites (produce twice as many offspring) for a nuclear male sterility gene to become established (Lewis, 1941). However, cytoplasmic male sterility can become established when the fertility of the female is only slightly larger than that of the hermaphrodite (Lewis, 1941). This is because a cytoplasmic gene is not inherited through male function hence has nothing to lose if pollen production is stopped. In some species, male sterility is complicated further by the evolution of restorer genes which suppress the deleterious effects of cytoplasmic male sterility (Schnable and Wise, 1998).

Most previous models of inherited male sterility assumed that female fitness is dependent on the availability of pollen in the environment but hermaphrodite fitness is not (Lewis, 1941; Lloyd, 1983), i. e. hermaphrodites are self-compatible. However, incompatibility recognition systems preventing self-fertilization have evolved several times in independent lineages of Angiosperm plants (Charlesworth et al., 2005) and many plants have been observed as self-incompatible (Igic and Kohn, 2006). If the case of a self-incompatible species is considered, cytoplasmic inherited male sterility is only stable if hermaphrodite and female fertility are exactly equal (Charnov, 1982). In this unlikely case it would be difficult for the cytoplasmic mutation to invade from small frequencies as it is neutral in terms of selection. For the case of cytoplasmic male sterility in out-crossing hermaphrodites, it was shown that if female fertility is larger than hermaphrodite fertility, females will spread until scarcity of pollen causes the population to become extinct (Stewart-Cox et al., 2005).

All of the analyses discussed thus far ignore spatial detail, which becomes

3

44 important in populations with short range interactions between constituents
45 and limited mixing caused by poor/no locomotion. These conditions would
46 be expected to be particularly prevalent in plant populations. A powerful ap-
47 proach for modelling spatial detail is the use of stochastic spatial simulations,
48 which have been extensively applied in chemical, ecological and sociological
49 systems (Durrett, 1999; Durrett and Levin, 1994).

50 A spatial model of cytoplasmic male sterility in self-incompatible herm-
51 aphrodites (Stewart-Cox et al., 2005), showed behaviour vastly different from
52 the predictions of non-spatial models. Where non-spatial models predicted
53 that invasion of females would lead to extinction of the population (female
54 fertility > hermaphrodite fertility), the spatial model (Stewart-Cox et al.,
55 2005) instead displayed stable nodes, foci, limit cycles or extinction depend-
56 ing on the relative fertility of females to hermaphrodites. This demonstrated
57 that cytoplasmic male sterility can evolve in self-incompatible hermaphrodite
58 populations.

59 In this article we present a generalised model for gynodioecy that accom-
60 modates male sterility conferred by a cytoplasmic gene or a dominant allele
61 in a nuclear gene. This contrasts the aforementioned spatial investigation
62 (Stewart-Cox et al., 2005), which solely considered cytoplasmic male steril-
63 ity. We present a generalised mean-field analysis (which ignores any spatial
64 detail), together with stochastic spatial simulations, to investigate the spatial
65 effect on the evolution of gynodioecy in self-incompatible hermaphrodites.

66 For established gynodioecious populations we compare the equilibrium
67 frequencies of females in spatial and non-spatial models over a range of pa-
68 rameter values. A knowledge of the equilibrium frequency of females would

4

₆₉ be of interest when comparing the results of breeding experiments with ob-

₇₀ servations of female frequency in the wild.

₇₁ In the following section a stochastic spatial simulation is described that

₇₂ is used to simulate the evolution of gynodioecy. A mean-field analysis for

₇₃ the evolution of gynodioecy is presented in section 3 and results from the

₇₄ stochastic spatial simulations are presented in section 4. The results pre-

₇₅ sented for the case of cytoplasmic male sterility show good agreement with

₇₆ previous spatial simulations (Stewart-Cox et al., 2005).

2. Model

₇₈ The stochastic spatial simulation described here is continuous in time

₇₉ and extends a previous model for the sexual reproductive process (Preece

₈₀ and Mao, 2009). The population resides on a two-dimensional square lattice

₈₁ of side length L, with periodic boundary conditions. Each lattice site can be

₈₂ occupied by either a self-incompatible hermaphrodite, a female or be empty.

₈₃ An occupied site becomes vacant at a rate λ, the death rate. The death rate

₈₄ is considered to be equal for hermaphrodites and females for the purposes of

₈₅ our investigation.

₈₆ A hermaphrodite produces an offspring at a rate equal to $j\kappa_1/4$, where j

₈₇ is the number of nearest neighbour sites occupied by hermaphrodites and κ_1

₈₈ is the birth rate. This positive relationship between individual fitness and the

₈₉ density of conspecifics demonstrates the well-known Allee effect(Odum and

₉₀ Allee, 1954). A nearest neighbour site is then chosen randomly. If the chosen

₉₁ site is empty the offspring is placed on the site. If the site is occupied the

₉₂ offspring is deleted. Similarly, a female produces a hermaphrodite offspring

5

93 at a rate, $j\kappa_2/4$, and a female offspring at a rate, $j\kappa_3/4$. Thus, a female

94 produces offspring at a total rate, $j(\kappa_2 + \kappa_3)/4$.

95   Genetics can be explicitly defined in this model for the case of a dominant

96 allele in a nuclear gene that causes male sterility, or a cytoplasmic gene that

97 causes male sterility. Consider a dominant nuclear allele for male sterility,

98 B. Thus, Bb = female, and, bb = hermaphrodite. Since females produce no

99 pollen, no homozygous BB individuals are formed and there are only two

100 genotypes in the population (Lewis, 1941). $\kappa_2 \neq \kappa_3$, represents the case of

101 differential mortality between male and female offspring due to their own sex

102 genotypes (Lloyd, 1974).

103   The case of cytoplasmic male sterility is modelled by setting $\kappa_2 = 0$.

104 Hence, females always produce females and the hermaphrodite population is

105 not increased through mating with females.

106 **3. Mean-field Analysis**

107   The mean-field kinetics of the hermaphrodite and female populations are

108 described by,

$$\frac{dh}{dt} = h\left[-\lambda + \frac{3\left(h\kappa_1 + f\kappa_2\right)\left(1 - h - f\right)}{4}\right] \qquad (1)$$

$$\frac{df}{dt} = f\left[-\lambda + \frac{3h\kappa_3\left(1 - h - f\right)}{4}\right] \qquad (2)$$

109 where h and f are the densities of hermaphrodites and females respectively.

110 The derivation of equations (1) and (2) is explained in appendix A. By scaling

111 time ($\tau = \lambda t$), the system can be simplified by introducing the parameters;

112 $K_1 = 3\kappa_1/4\lambda$, $K_2 = 3\kappa_2/4\lambda$ and $K_3 = 3\kappa_3/4\lambda$.

6

In the following mean-field analysis, the case of nuclear male sterility $(K_1 > 0,\ K_2 > 0\ \text{and}\ K_3 > 0)$ will be considered first and the case of cytoplasmic male sterility $(K_1 > 0,\ K_2 = 0\ \text{and}\ K_3 > 0)$ will be considered second.

3.1. Nuclear male sterility.

Equilibria for equations (1) and (2) were found by setting the time derivative equal to zero, then solving the resulting two equations simultaneously. The nature of these equilibria was characterised by linear stability analysis of the system of equations (1) and (2). As $h \geq 0$, $f \geq 0$ and $h + f \leq 1$, the region of interest on the (h,f)-plane is the triangle with vertices $(h = 0, f = 0)$, $(h = 1, f = 0)$ and $(h = 0, f = 1)$. The trivial equilibrium $(h = 0, f = 0)$ is stable provided $\lambda > 0$. For $(K_1 > 0, K_2 > 0, K_3 > 0)$, equations (1) and (2) have four equilibria besides the trivial one. Two equilibria are located on the boundary $(f = 0)$ with,

$$h_2 = \frac{1}{2}\left(1 - \sqrt{\frac{K_1 - 4}{K_1}}\right), \tag{3}$$

$$h_3 = \frac{1}{2}\left(1 + \sqrt{\frac{K_1 - 4}{K_1}}\right). \tag{4}$$

The remaining two equilibria are,

$$h_4 = \frac{K_2 K_3 - \sqrt{A}}{2K_3\left(K_2 + K_3 - K_1\right)}, \tag{5}$$

$$f_4 = \frac{\left(K_3 - K_1\right)\left(K_2 K_3 - \sqrt{A}\right)}{2K_2 K_3\left(K_2 + K_3 - K_1\right)}, \tag{6}$$

$$h_5 = \frac{K_2 K_3 + \sqrt{A}}{2K_3\left(K_2 + K_3 - K_1\right)}, \tag{7}$$

7

$$f_5 \;=\; \frac{(K_3 - K_1)\left(K_2 K_3 + \sqrt{A}\right)}{2 K_2 K_3 \left(K_2 + K_3 - K_1\right)}, \tag{8}$$

128 where $A = K_2 K_3 \left[4\left(K_1 - K_2 - K_3\right) + K_2 K_3\right]$. Eigenvalues and eigenvectors

129 from the linear stability analysis of these equilibria can be found in appendix

130 B.

131   Equilibria $(h_2, 0)$ and $(h_3, 0)$ are real and positive only if $K_1 > 4$. The

132 eigenvalues from the linear stability analysis of these equilibria are only de-

133 pendent on K_1 and K_3 (see appendix B). If $K_1 > K_3$, equilibria $(h_2, 0)$ and

134 $(h_3, 0)$ are a saddle point and attractor respectively. This marks a regime

135 where hermaphroditism is an ESS. Thus, a small number of mutant females

136 cannot invade a hermaphrodite population. Later it will be shown that when

137 $K_1 > K_3$, only equilibria $(0, 0)$, $(h_2, 0)$ and $(h_3, 0)$ exist in the region of inter-

138 est. Typical mean-field dynamics for the regime, where $K_1 > 4$ and $K_1 > K_3$,

139 are shown in figure 1. The unstable manifold of the saddle point in figure 1

140 lies along the boundary $(f = 0)$. Thus, a population of just hermaphrodites

141 evolves to the trivial equilibrium if the initial density of the population is

142 below the saddle point and evolves to the stable node if the initial density of

143 the population is above the saddle point.

144   If $K_3 > K_1$, equilibria $(h_2, 0)$ and $(h_3, 0)$ are an unstable node and saddle

145 point respectively. The unstable manifold of the saddle point at $(h_3, 0)$ points

146 in to the interior, $(h > 0, f > 0)$. In the absence of females the dynamics of

147 the hermaphrodite population is the same as for the case, $K_1 > K_3$. How-

148 ever, a small number of mutant females can now invade the hermaphrodite

149 population. Thus, Hermaphroditism is no longer an ESS.

150   By inspecting equations (5)-(8) it can be seen that equilibria (h_4, f_4) and

8

151 (h_5, f_5) are real only if $A \geq 0$. Using this condition, it can be shown that
152 equilibria (h_4, f_4) and (h_5, f_5) are positive, real, and distinct if,

$$K_3 > 4,$$

$$K_3 > K_1,$$

$$\text{and} \quad K_2 > S, \tag{9}$$

153 where,

$$S = \frac{4K_3 - 4K_1}{K_3 - 4}. \tag{10}$$

154 When they exist in the region of interest, equilibria (h_4, f_4) and (h_5, f_5) are
155 a saddle point and stable node respectively. The condition, in equation (9),
156 that $K_3 > K_1$, means that the boundary equilibria $(h_2, 0)$ and $(h_3, 0)$ are an
157 unstable node and a saddle point respectively. Typical mean-field dynamics
158 for this regime are shown in figure (2). In the absence of females, the dy-
159 namics of hermaphrodite population is similar to the case where $K_1 > K_3$:
160 a population of just hermaphrodites evolves to the trivial equilibrium if the
161 initial density of hermaphrodites is below the unstable node and evolves to
162 the boundary saddle point if the initial density of hermaphrodites is above
163 the unstable node. However, females can now invade a population of herm-
164 aphrodites. The population can then evolve to the stable node (h_5, f_5), which
165 represents a stable coexisting population of hermaphrodites and females. As
166 can be seen in figure(2), mixed populations with low densities evolve to the
167 trivial equilibrium.

168   The conditions in equations (9) also reveal that a coexisting population of
169 females and hermaphrodites can be stable even when a population consisting
170 solely of hermaphrodites is not stable (when $K_1 < 4$).

9

171 Whilst obeying equations (9), reducing K_3 (or increasing K_1) brings equi-

172 libria (h_4, f_4) and (h_5, f_5) closer to the boundary ($f = 0$). When $K_3 = K_1$,

173 equilibria (h_4, f_4) and (h_5, f_5) collide with the boundary equilibria, $(h_2, 0)$

174 and $(h_3, 0)$ respectively, here a transcritical bifurcation occurs. As discussed

175 above, when $K_1 > K_3$, the boundary equilibria $(h_2, 0)$ and $(h_3, 0)$ are a saddle

176 point and attractor respectively. Thus hermaphroditism is the ESS.

177 Decreasing K_2, whilst obeying the conditions in equation 9, brings equi-

178 libria (h_4, f_4) and (h_5, f_5) closer together. At $K_2 = S$, equilibria (h_4, f_4) and

179 (h_5, f_5) collide and annihilate. This is a saddle-node bifurcation point. If

180 $K_3 > K_1$ and $K_2 < S$; the boundary equilibria, $(h_2, 0)$ and $(h_3, 0)$, are a

181 node and saddle point respectively and no equilibrium for coexistence exists.

182 Under these conditions females could invade the hermaphrodite population.

183 As the only stable equilibrium is the trivial equilibrium the population will

184 then converge on the trivial equilibrium, resulting in extinction. Typical

185 mean-field dynamics for this regime are shown in figure 3.

186 All possible evolutionary outcomes for the case $K_1 > 0$, $K_2 > 0$ and

187 $K_3 > 0$ are summarised in table (1). At equilibrium the frequency of females

188 in the population is given by,

$$\frac{f_5}{f_5 + h_5} = \frac{K_3 - K_1}{K_3 + K_2 - K_1}. \tag{11}$$

189 Note that equation (11) is only valid if the (h_5, f_5) is real and positive, there-

190 fore if the conditions in equation 9 are satisfied. Equation 11 differs from the

191 result of Lewis (1941) as Lewis's model considers self-compatible hermaph-

192 rodites.

10

	$K_1 > 4$	$K_1 < 4$
$K_1 > K_3$	Hermaphroditism is ESS	Extinction (only trivial equilibrium)
$(K_3 > K_1)$ & $(S > K_2)$	Female invasion leads to extinction	Extinction (only trivial equilibrium)
$(K_3 > K_1)$ & $(K_2 > S)$ & $(K_3 > 4)$	Gynodioecy	Gynodioecy

Table 1: Evolutionary outcomes in mean-field analysis, for nuclear male sterility ($K_1 > 0, K_2 > 0, K_3 > 0$), where K_1, K_2 and K_3 are the scaled reproductive rates for the following processes: $H + H \to H$, $H + F \to H$, and $H + F \to F$ respectively (H represents a hermaphrodite and F a female).

3.2. Cytoplasmic male sterility

For the case of cytoplasmic male sterility, the behaviour of equilibria $(h_2, 0)$ and $(h_3, 0)$ is the same as in the previous section: for $K_1 > K_3$ equilibria $(h_2, 0)$ and $(h_3, 0)$ are a a saddle point and stable node respectively, for $K_3 < K_1$ equilibria $(h_2, 0)$ and $(h_3, 0)$ are an unstable node and saddle point respectively.

If $K_2 = 0$ and $K_1 > K_3$, hermaphroditism is an ESS and similar dynamics to those shown in figure 1 are observed. For $K_2 = 0$ and $K_3 > K_1$, females can invade a hermaphrodite population but the population then converges on the trivial equilibria and becomes extinct. The dynamics observed for this case are similar to those shown in figure 3.

For the special case $K_2 = 0$ and $K_3 = K_1$, there is a curve of equilibrium

11

205 points given by,

$$f = \frac{K_1 h - K_1 h^2 - 1}{K_1 h}. \tag{12}$$

206 Eigenvalues and eigenvectors from the linear stability analysis of this equi-

207 librium curve are given in appendix C. The first eigenvalue for points on this

208 equilibrium curve is zero with corresponding eigenvector along the curve.

209 The second eigenvalue is negative for $h > 2/K_1$ and positive for $h < 2/K_1$.

210 Typical mean-field dynamics for this regime is shown in figure 4. The be-

211 haviour observed here for the case $K_2 = 0$ is in agreement with previous

212 results from similar evolutionary models (Stewart-Cox et al., 2005; Charnov,

213 1982).

214 4. Results of lattice simulation

215   All simulations were run on lattices of side length $L = 100$ for 100 gen-

216 erations, where the time in generations is given by $\tau = \lambda t$, and t is in Monte

217 Carlo steps. For hermaphrodite populations (with no females), previous in-

218 vestigations for this lattice model (Preece and Mao, 2009) have shown that a

219 discontinuous phase transition occurs between an active phase (finite popula-

220 tion) and an absorbing phase (extinction) at $K_1 \approx 6$. Thus values of $K_1 > 6$

221 are required for a sustainable hermaphrodite population.

222   The simulation results for the case of cytoplasmic male sterility ($K_2 = 0$)

223 show good qualitative agreement with previous spatial simulations (Stewart-

224 Cox et al., 2005). Simulations (for $K_2 = 0$) displayed coexistence of females

225 and hermaphrodites (not shown) for values of K_3 roughly 1.5 times lager than

226 K_1. Figure 5 shows how behaviour is increasingly cyclic with increased female

227 reproductive advantage (increased K_3/K_1). This contrasts with mean-field

12

₂₂₈ kinetics, which predict extinction of the population following the invasion
₂₂₉ of females. Large vales of K_3 ($K_3 > 8K_1$) result in extinction (not shown)
₂₃₀ showing similar behaviour to mean-field predictions.

₂₃₁   Sample paths from the lattice simulation for the case of nuclear male
₂₃₂ sterility ($K_2 > 0$) are shown in figures 6 and 7. In figure 6, hermaphroditism
₂₃₃ is the ESS. It can be seen from the plot, that the hermaphrodite population
₂₃₄ is robust against invasion by large numbers of females. Simulations started
₂₃₅ with low population densities evolved to the trivial equilibrium (not shown).
₂₃₆ These observations are in agreement with mean-field kinetics. In figure 7,
₂₃₇ coexistence of females and hermaphrodites is evolutionary stable. The paths
₂₃₈ shown in figure 7 converge on an equilibrium at approximately $(0.77, 0.12)$,
₂₃₉ this corresponds to the stable node, (h_5, f_5), in the mean-field analysis. This
₂₄₀ is difficult to see from figure 7 due to slow dynamics close to the equilibrium.
₂₄₁ Simulations started with low population densities evolved to the trivial equi-
₂₄₂ librium (not shown).

₂₄₃   Breaking the condition $K_2 > S$ (equation (9)) with $K_3 > K_1$ does not
₂₄₄ result in extinction following female invasion, as predicted by mean-field
₂₄₅ analysis. Instead simulations display coexistence with increasingly cyclic be-
₂₄₆ haviour as K_2 is decreased and/or K_3 increased. This result is not surprising
₂₄₇ given the observations for $K_2 = 0$ shown earlier (figure 5).

₂₄₈   The frequency of females in natural gynodioecious populations is often
₂₄₉ used as an indicator of the genetic mechanism responsible for male steril-
₂₅₀ ity in a particular species (Bailey and Delph, 2007). For cases of nuclear
₂₅₁ male sterility where $K_2 > S$, spatial simulations arrive at equilibria which
₂₅₂ are fairly static in (h, f)-space. Thus, equilibrium frequencies of females in

13

the population are easily calculated. Figure 8 plots the equilibrium female frequencies for spatial simulation and mean-field analysis as a function of K_3/K_1, with $K_2 = K_3$. For each set of results K_1 was fixed while K_2 and K_3 were incremented. By testing several values of K_1, the plots show that the relative magnitudes of K_1, K_2 and K_3 are dominant in determining the behaviour of the system and not their absolute values. Though birth rates do need to be of sufficient magnitude to avoid extinction. Reproductive rates used for the simulations in figures 5–8 are larger than those use for mean-field dynamics (figures 1–4). This because the strictly local interactions of the simulation make the population more vulnerable to extinction at low birth rates (Preece and Mao, 2009).

Mean-field analysis predicted that nuclear male sterility could evolve if $K_3 > K_1$. Figure 8 shows that the condition for nuclear male sterility to evolve in a spatial simulation with ($K_2 = K_3$) is approximately $K_3 > 3K_1$. This infers that nuclear male sterility is less likely to evolve in species with local pollination and seed setting, as is the case in the simulation, than in than in a well mixed/widely dispersing population. Results from lattice simulations are summarised in table 2.

Figure 8 also shows that female frequency is lower in the spatial simulation than predicted by mean-field analysis. Thus, it may be expected that gynodioecious plant species with local pollination and seed setting should have lower female frequencies in the wild compared to species with long range interactions. The difference between mean-field and simulation is likely to be due to local variation in the concentration of females. As offspring are placed on nearest neighbour sites females with easy access to pollen can-

14

Male Sterility	Parameters	Evolutionary Outcome
Nuclear	$3K_1 > K_3$ & $K_3 = K_2$	Hermaphroditism is ESS
Nuclear	$K_3 > 3K_1$ & $K_3 = K_2$	Gynodioecy
Cytoplasmic	$1.5 > \frac{K_3}{K_1}$ & $K_2 = 0$	Hermaphroditism is ESS
Cytoplasmic	$8 > \frac{K_3}{K_1} > 1.5$ & $K_2 = 0$	Gynodioecy
Cytoplasmic	$\frac{K_3}{K_1} > 8$ & $K_2 = 0$	Female invasion leads to extinction

Table 2: Evolutionary outcomes for lattice simulations, where K_1, K_2 and K_3 are the scaled reproductive rates for the following processes: $H + H \rightarrow H$, $H + F \rightarrow H$, and $H + F \rightarrow F$ respectively (H represents a hermaphrodite and F a female). A value of $K_1 > 6$ is required for a sustainable hermaphrodite population.

²⁷⁸ not compensate for females being starved of pollen in regions of high female

²⁷⁹ concentration. This would result in regions with high female concentration

²⁸⁰ dying off due to a shortage of pollen.

²⁸¹ In many hermaphrodite plant populations individuals are self-incompatible

²⁸² (Igic and Kohn, 2006), which is the focus of the model presented above. In

²⁸³ other species some self-fertilisation is observed in addition to out-crossing

²⁸⁴ (Kohn, 1989; Ashman, 1999). Though selfing would alter the details of the

²⁸⁵ model presented in this article, we would still expect the main conclusions

²⁸⁶ of our investigation to stand. Namely, females require a greater fertility

²⁸⁷ advantage to become established when interactions are local, and the equi-

²⁸⁸ librium frequency of females is lower when interactions are local. This may

²⁸⁹ account for observations of Ashman (1999) that observed female frequencies

²⁹⁰ are generally lower than those predicted by the equation of Lewis (1941) in

15

a gynodioecious species of wild strawberry.

As pointed out in the introduction, male sterility has also been observed to be controlled by more complex genetic interactions than studied here. For example male sterility due to recessive genes (Lewis, 1941) and the evolution of restorer genes which counter male sterility (Schnable and Wise, 1998). Spatial simulations similar to the one presented here could easily be applied to these systems.

5. Conclusions

The population dynamics for a stochastic spatial simulation and its mean-field approximation have been presented for a gynodioecious population where male sterility is conferred by a dominant nuclear allele. It was demonstrated that a female needs a much greater fertility advantage to become established in the stochastic spatial simulation when compared with the mean-field approximation. This result suggests that gynodioecy is less likely to evolve in plants with local pollination and seed setting, and may also contribute to the observation that a relatively small percentage of plant species exhibit gynodioecy (Richards, 1986) and dioecy (Dellaporta and Calderonurrea, 1993).

The equilibrium frequency of females in the population was found to be lower in the stochastic spatial simulation than in the mean-field approximation. This suggests that a lower frequency of females should be expected for gynodioecious populations with local pollination and seed setting.

16

6. Acknowledgements

A. Derivation of mean-field dynamics

According to the reproductive process described in section 2, a hermaphrodite produces offspring via its female sexual function at a mean rate,

$$r = \frac{\kappa_1}{4} \sum_{j=0}^{4} [j\mathbf{P}(j)\mathbf{P}(x = \oslash|j)], \tag{13}$$

where j is the number of nearest neighbour sites occupied by hermaphrodites, κ_1 is the birth rate, $\mathbf{P}(j)$ is the probability a hermaphrodite has j nearest neighbours, and $\mathbf{P}(x = \oslash|j)$ is the probability that the site chosen for the offspring to reside on, x, is empty given j nearest neighbour sites are occupied by hermaphrodites. Applying Bayes' theorem to equation(13),

$$r = \frac{\kappa_1}{4} \sum_{j=0}^{4} [j\mathbf{P}(x = \oslash)\mathbf{P}(j|x = \oslash)]. \tag{14}$$

As $\mathbf{P}(x = \oslash)$ is not a function of j it can be taken out of sum in equation(14) and placed as a prefactor. In the meanfield,

$$\mathbf{P}(x = \oslash) = (1 - h - f), \tag{15}$$

where h and f are the densities of hermaphrodites and females respectively. In the meanfield, the remaining sum from equation (14) is,

$$\sum_{j=0}^{4} [j\mathbf{P}(j|x = \oslash)] = 3h. \tag{16}$$

17

328 The factor of 3 arises because $\mathbf{P}\left(j|x=\oslash\right)=0$ for $j=4$. Substituting

329 equations(15) and (16) into equation(13) gives,

$$r = \frac{3h\left(1-h-f\right)}{4}. \tag{17}$$

330 Equation(17) is the meanfield reproductive rate per hermaphrodite via its

331 female sexual function. A similar derivation can be used to calculate the

332 meanfield rates that hermaphrodites and females are produced by female

333 individuals.

B. Stability analysis — nuclear male sterility

335 The equilibrium points for nuclear male sterility are given in equations

336 (3) – (8). The eigenvalues for the trivial equilibrium $(0,0)$ are,

$$\nu_1^1 = -1, \tag{18}$$

$$\nu_1^2 = -1, \tag{19}$$

337 with corresponding eigenvectors,

$$\mathbf{z_1^1} = (0,1), \tag{20}$$

$$\mathbf{z_1^2} = (1,0). \tag{21}$$

338 The eigenvalues for $(h_2,0)$ are,

$$\nu_2^1 = \frac{4-K_1+\sqrt{K_1\left(K_1-4\right)}}{2}, \tag{22}$$

$$\nu_2^2 = \frac{K_3}{K_1}-1, \tag{23}$$

339 with corresponding eigenvectors,

$$\mathbf{z_2^1} = (1,0), \tag{24}$$

18

$$\mathbf{z_2^2} \;=\; \left(\frac{K_1 \left(2 - K_1 + \sqrt{K_1 \left(K_1 - 4 \right)} \right) + 2K_2}{K_1 \left(K_1 - 6 - \sqrt{K_1 \left(K_1 - 4 \right)} \right) + 2K_3}, 1 \right). \tag{25}$$

The eigenvalues for $(h_3, 0)$ are,

$$\nu_3^1 \;=\; \frac{4 - K_1 - \sqrt{K_1 \left(K_1 - 4 \right)}}{2}, \tag{26}$$

$$\nu_3^2 \;=\; \frac{K_3}{K_1} - 1, \tag{27}$$

with corresponding eigenvectors,

$$\mathbf{z_3^1} \;=\; (1, 0) \tag{28}$$

$$\mathbf{z_3^2} \;=\; \left(\frac{K_1 \left(2 - K_1 - \sqrt{K_1 \left(K_1 - 4 \right)} \right) + 2K_2}{K_1 \left(K_1 - 6 + \sqrt{K_1 \left(K_1 - 4 \right)} \right) + 2K_3}, 1 \right). \tag{29}$$

The eigenvalues of $(h_4, 0)$ are,

$$\nu_4^1 \;=\; \frac{K_1}{K_3} - 1, \tag{30}$$

$$\nu_4^2 \;=\; \frac{2}{1 + K_2 K_3 A^{-1/2}}, \tag{31}$$

where $A = K_2 K_3 \left[4 \left(K_1 - K_2 - K_3 \right) + K_2 K_3 \right]$. The corresponding eigenvectors are,

$$\mathbf{z_4^1} \;=\; \left(\frac{-K_2 \left(2K_1 + K_2 \left(K_3 - 2 \right) - 4K_3 + A^{1/2} \right)}{K_3 \left(2K_1 + K_2 \left(K_3 - 4 \right) - 2K_3 + A^{1/2} \right)}, 1 \right), \tag{32}$$

$$\mathbf{z_4^2} \;=\; \left(\frac{K_2}{K_3 - K_1}, 1 \right). \tag{33}$$

The eigenvalues of $(h_5, 0)$ are,

$$\nu_5^1 \;=\; \frac{K_1}{K_3} - 1, \tag{34}$$

$$\nu_5^2 \;=\; \frac{2}{1 - K_2 K_3 A^{-1/2}}, \tag{35}$$

19

where the corresponding eigenvectors are,

$$
\mathbf{z_5^1} = \left(\frac{-K_2 \left(2K_1 + K_2 \left(K_3 - 2 \right) - 4K_3 - A^{1/2} \right)}{K_3 \left(2K_1 + K_2 \left(K_3 - 4 \right) - 2K_3 - A^{1/2} \right)}, 1 \right), \tag{36}
$$

$$
\mathbf{z_5^2} = \left(\frac{K_2}{K_3 - K_1}, 1 \right). \tag{37}
$$

C. Stability analysis — cytoplasmic male sterility

$(h_2,0)$ and $(h_3,0)$ are still equilibria for the case of cytoplasmic male sterility ($K_1 > 0$, $K_2 = 0$ and $K_3 > 0$). Though, (h_4,f_4) and (h_5,f_5) are not. For the special case $K_3 = K_1$, a curve of equilibrium points exists given by equation (12). The eigenvalues from the linear stability analysis of points on this curve are given by,

$$
\nu_6^1 = 0, \tag{38}
$$

$$
\nu_6^2 = 2 - K_1 h, \tag{39}
$$

where the hermaphrodite density h refers to the hermaphrodite density on the equilibrium curve. The corresponding eigenvectors are,

$$
\mathbf{z_6^1} = \left(\frac{K_1 h^2}{1 - K_1 h^2}, 1 \right), \tag{40}
$$

$$
\mathbf{z_6^2} = \left(\frac{-K_1 h^2}{1 + K_1 h \left(h - 1 \right)}, 1 \right), \tag{41}
$$

again the hermaphrodite density h refers to the hermaphrodite density on the equilibrium curve.

References

Ashman, T. L., Jul. 1999. Determinants of sex allocation in a gynodioecious wild strawberry: implications for the evolution of dioecy and sexual dimorphism. Journal Of Evolutionary Biology 12 (4), 648–661.

20

361 Bailey, M. F., Delph, L. F., 2007. A field guide to models of sex-ratio evolu-
362   tion in gynodioecious species. Oikos 116, 1609–1617.

363 Charlesworth, D., Vekemans, X., Castric, V., Glemin, S., 2005. Plant self-
364   incompatibility systems: a molecular evolutionary perspective. New Phy-
365   tologist 168 (1), 61–69.

366 Charnov, E. L., 1982. The Theory of Sex Allocation. Princeton University
367   Press.

368 Chaudhury, A. M., Oct. 1993. Nuclear genes-controlling male-fertility. Plant
369   Cell 5 (10), 1277–1283.

370 Dellaporta, S. L., Calderonurrea, A., Oct. 1993. Sex determination in flow-
371   ering plants. Plant Cell 5 (10), 1241–1251.

372 Durrett, R., Dec. 1999. Stochastic spatial models. SIAM Review 41 (4), 677–
373   718.

374 Durrett, R., Levin, S. A., Feb. 1994. Stochastic spatial models a users guide
375   to ecological applications. Philosophical Transactions of the Royal Society
376   of London Series B — Biological Sciences 343 (1305), 329–350.

377 Igic, B., Kohn, J. R., 2006. The distribution of plant mating systems: Study
378   bias against obligately outcrossing species. Evolution 60 (5), 1098–1103.

379 Kohn, J. R., 1989. Sex-ratio, seed production, biomass allocation, and the
380   cost of male function in cucurbita-foetidissima (cucurbitaceae). Evolution
381   43 (7), 1424–1434.

382 Lewis, D., 1941. Male sterility in natural populations of hermaphrodite
383 plants. New Phytologist 40, 56–63.

384 Lloyd, D. G., 1974. Theoretical sex-ratios of dioecious and gynodioecious
385 angiosperms. Heredity 32 (FEB), 11–34.

386 Lloyd, D. G., 1983. Evolutionarily stable sex-ratios and sex allocations. Jour-
387 nal of Theoretical Biology 105 (3), 525–539.

388 Obeso, J. R., Alvarez-Santullano, M., Retuerto, R., Nov. 1998. Sex ra-
389 tios, size distributions, and sexual dimorphism in the dioecious tree ilex
390 aquifolium (aquifoliaceae). American Journal Of Botany 85 (11), 1602–
391 1608.

392 Odum, H. T., Allee, W. C., 1954. A note on the stable point of populations
393 showing both intraspecific cooperation and disoperation. Ecology 35 (1),
394 95–97.

395 Preece, T., Mao, Y., 2009. Sustainability of dioecious and herm-
396 aphrodite populations on a lattice. Journal of Theoretical Biology,
397 doi:10.1016/j.jtbi.2009.08.009.

398 Richards, A., 1986. Plant breeding systems. George Allen and Unwin, Lon-
399 don.

400 Schnable, P. S., Wise, R. P., 1998. The molecular basis of cytoplasmic male
401 sterility and fertility restoration. Trends in Plant Science 3, 175–180.

402 Stewart-Cox, J. A., Britton, N. F., Mogie, M., Nov. 2005. Space mediates co-

[403] existence of females and hermaphrodites. Bulletin of Mathematical Biology
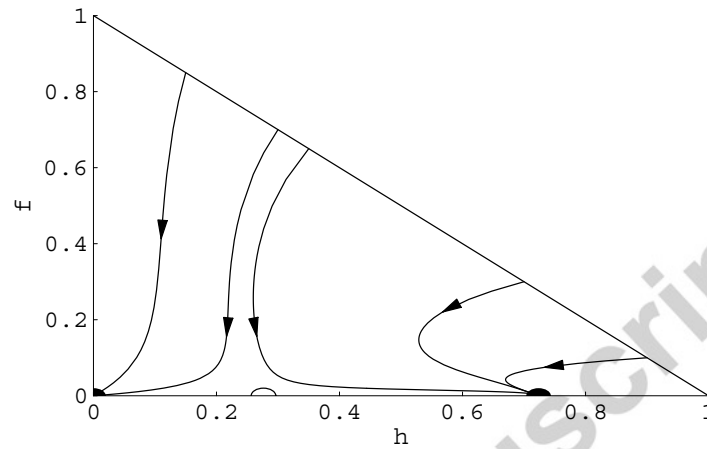[404] 67 (6), 1273–1302.

Figure 1: Typical mean-field dynamics for the case where hermaphroditism is the ESS. Filled circles mark stable nodes, the empty circle marks a saddle point. The arrows indicate the direction of evolution. Plot shown for $K_1 = 5$, $K_2 = 3$ and $K_3 = 3$.
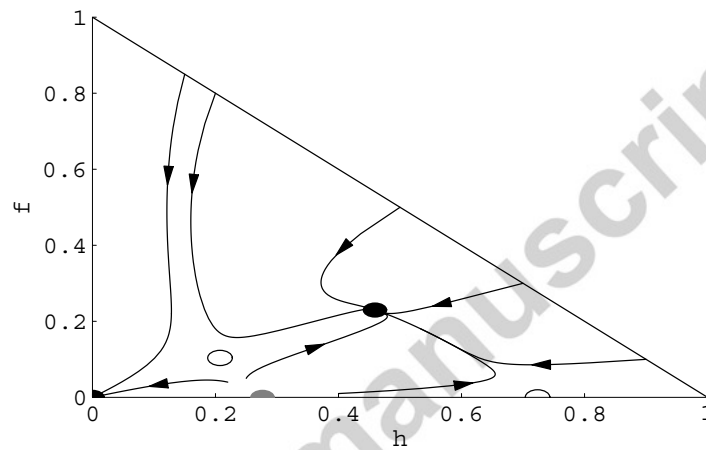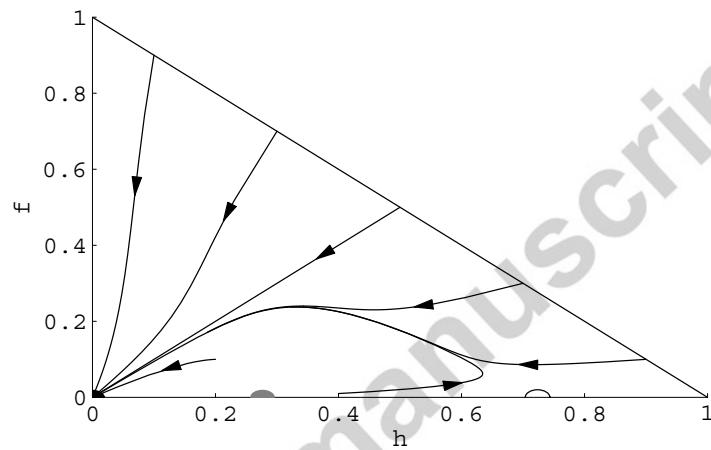
Figure 2: Typical mean-field dynamics for the case where a coexisting population of hermaphrodites and females is evolutionary stable. Filled circles mark stable nodes, empty circles mark saddle points and the grey filled circle marks an unstable node. The arrows indicate the direction of evolution. Plot shown for $K_1 = 5$, $K_2 = 4$ and $K_3 = 7$.
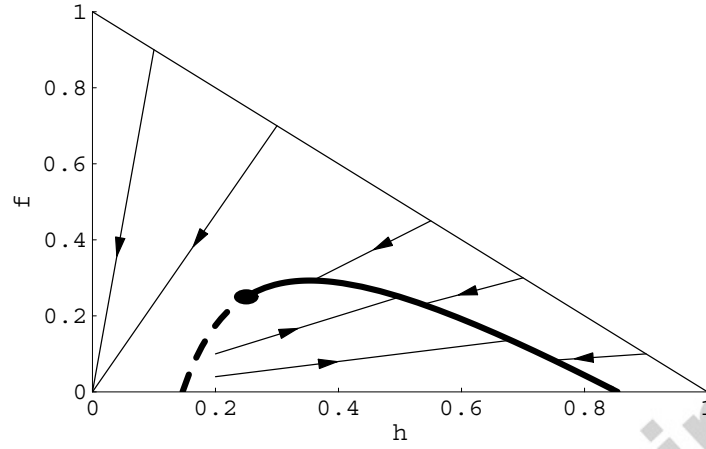
24

Figure 3: Typical mean-field dynamics for the case where invasion of females leads to extinction. Filled circles mark stable nodes, the empty circle marks a saddle points and the grey filled circle marks an unstable node. The arrows indicate the direction of evolution. Plot shown for $K_1 = 5$, $K_2 = 2$ and $K_3 = 7$.

Figure 4: Typical mean-field dynamics for the case where $K_1 = K_3$ and $K_2 = 0$. Plot shown for $K_1 = K_3 = 8$, $K_2 = 0$. The solid section of the curve is stable, the dashed section is unstable. The filled circle indicates the point at which the curve becomes unstable. The arrows indicate the direction of evolution.
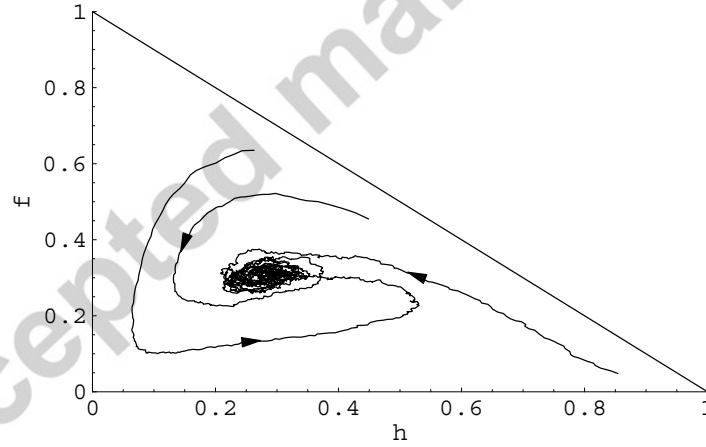

Figure 5: Lattice simulation for cytoplasmic male sterility; coexistence of females and hermaphrodites. The arrows indicate the direction of evolution. Simulations were run for 100 generations on a lattice of side length $L = 100$, with $K_1 = 10$, $K_2 = 0$ and $K_3 = 40$.
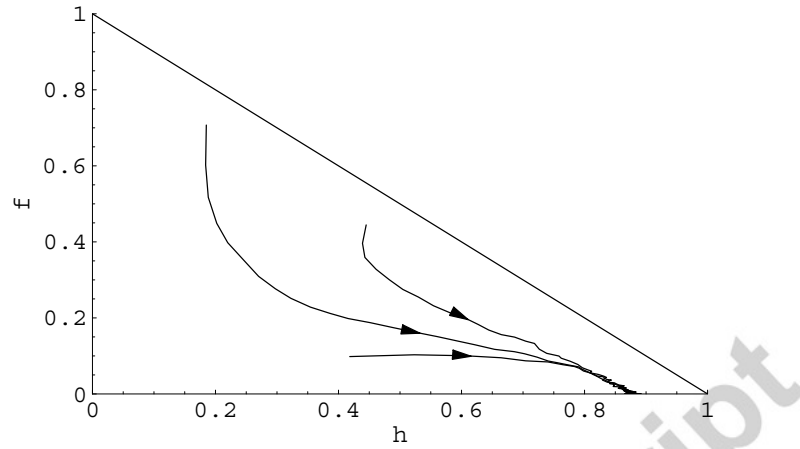
26

Figure 6: Lattice simulation; hermaphroditism is an ESS. The arrows indicate the direction of evolution. Simulations were run for 100 generations on a lattice of side length $L = 100$ with $K_1 = 10$, $K_2 = 8$ and $K_3 = 8$.
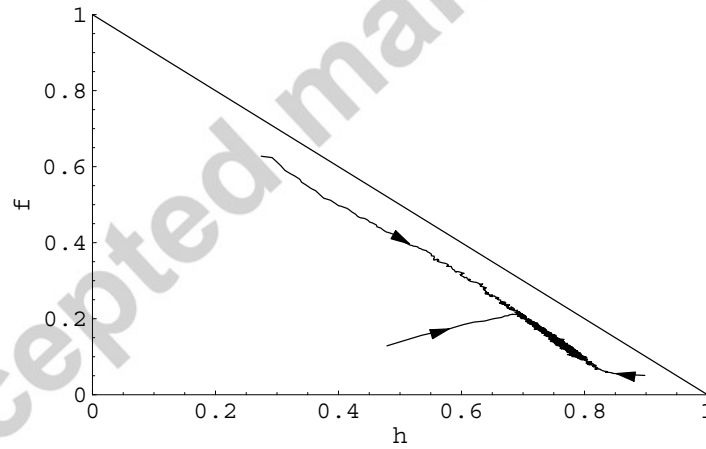

Figure 7: Lattice simulation; coexistence of females and hermaphrodites. The arrows indicate the direction of evolution. Simulations were run for 100 generations on a lattice of side length $L = 100$ with $K_1 = 10$, $K_2 = 40$ and $K_3 = 40$.
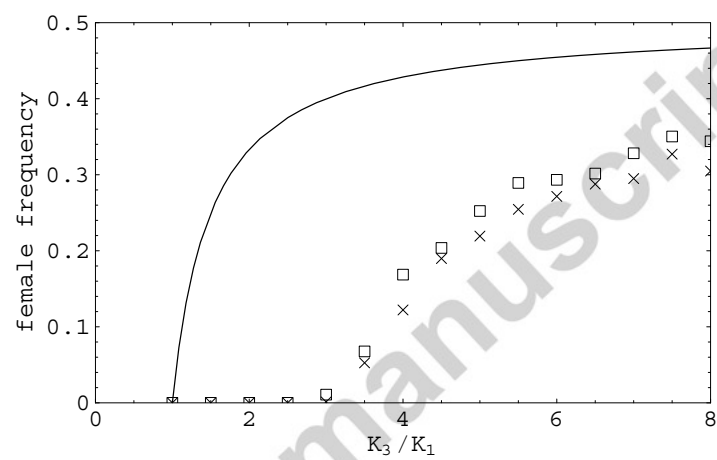
27

Figure 8: Comparison of equilibrium sex-ratio for mean-field (line) and lattice simulation. Simulations shown for $K_2 = K_3$, and $K_1 = 10$ (□) and $K_1 = 20$ (×). Points shown were averaged over the last 10 generations of the simulation.